Ternary Molybdenum Sulfide

$Ba_4Mo_{12}S_{18}$: A Superconductor Containing the Dimeric Unit $(Mo_6)_2S_{24}$, the Missing Link between the Mo_6S_{14} and Mo_9S_{17} Units

*Diala Salloum, Régis Gautier, Michel Potel, and Patrick Gougeon**

The ternary molybdenum chalcogenides $M_xMo_6X_8$ (M = Na, K, Ca, Sr, Ba, Sn, Pb, lanthanide, 3d element; X = S, Se, Te), known as Chevrel phases, have been studied intensively in the last three decades because of their exceptional physical properties.[1–4] Their crystal structure[5] consists of octahedral Mo_6 clusters surrounded by fourteen chalcogen atoms, eight of which form a distorted cube (*i*-type ligands), while the remaining six cap the faces of the X_8 cube (*a*-type ligands). In the formalism of Schäfer and von Schnering,[6] such a unit can be written as $Mo_6X_8^iX_6^a$. In the Chevrel phases, some of the chalcogen atoms of the $Mo_6X_8^iX_6^a$ unit are shared according to the developed formula $[Mo_6X_2^iX_{6/2}^{i-a}]X_{6/2}^{a-i}$ to form a three-dimensional Mo–X network. Different connectivities between the $Mo_6L_8^iL_6^a$ (L = Cl, Br, I, S, Se, Te) units leading to a variety of frameworks are known in reduced molybdenum halides and chalcohalides;[7] however, this occurrence in the Chevrel phases is the only one observed for the sulfides, selenides, and tellurides to date. Here we present the synthesis, crystal and electronic structures, and properties of an original reduced molybdenum sulfide, $Ba_4Mo_{12}S_{18}$, in which the $Mo_6S_8^iS_6^a$ units form the new dimeric unit $(Mo_6)_2S_{14}^iS^{i\text{-}i}S_3^{a\text{-}a}S_6^a$, which is the missing link between the $Mo_6S_8^iS_6^a$ unit and the $Mo_9S_{11}^iS_6^a$ unit containing the bioctahedral Mo_9 cluster.[8]

$Ba_4Mo_{12}S_{18}$ crystallizes in a new structural type, the three-dimensional Mo–S framework of which is based on the novel dimeric unit $(Mo_6)_2S_{14}^iS^{i\text{-}i}S_3^{a\text{-}a}S_6^a$ (Figure 1), which can be regarded as resulting from the fusion of two $Mo_6S_8^iS_6^a$ units by sharing two S^i and six S^a ligands, as shown in Figure 2 (left and middle). This new unit can be also viewed as an intermediate step towards the formation of the $Mo_9S_{11}^iS_6^a$ unit containing the bioctahedral Mo_9 cluster (Figure 2, right).[8] Halogens are well known to form *a*-*a* type ligands, however, this is the first time that sulfur atoms occupy such a position (S3 atom in Figure 3). The Mo_6 octahedra are more

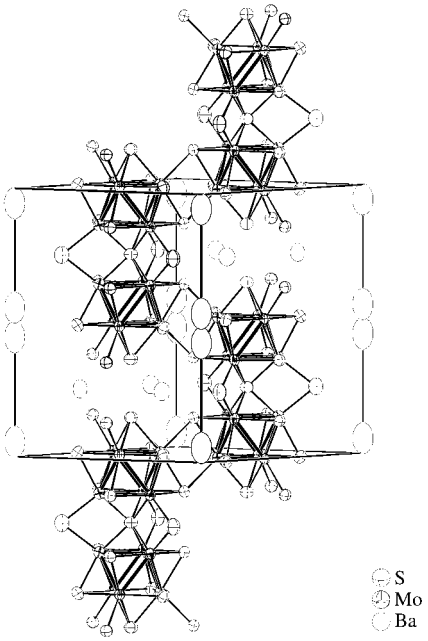

Figure 1. Crystal structure of $Ba_4Mo_{12}S_{18}$. Thick lines denote Mo–Mo bonds, and thin lines Mo–O bonds.

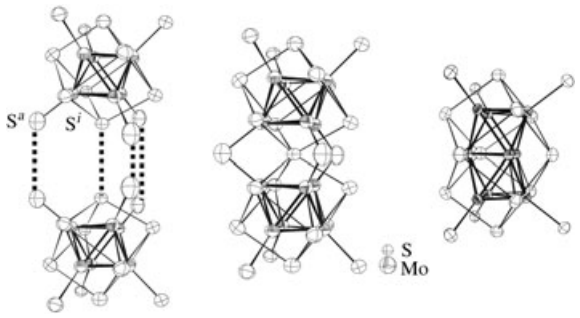

Figure 2. Process of formation of the $(Mo_6)_2S_{14}^iS^{i\text{-}i}S_3^{a-a}S_6^a$ unit (middle) from the fusion of two $Mo_6S_8^iS_6^a$ units (left). Right: the $Mo_9S_{11}^iS_6^a$ unit.

[*] D. Salloum, Dr. R. Gautier, Dr. M. Potel, Dr. P. Gougeon
CNRS, Université de Rennes 1, ENSC Rennes
Institut de Chimie de Rennes
Laboratoire de Chimie du Solide et Inorganique Moléculaire, UMR 6511
Avenue du Général Leclerc, 35042 Rennes Cedex (France)
Fax: (+33) 2-9963-5704
E-mail: patrick.gougeon@univ-rennes1.fr

 DOI: 10.1002/ange.200461255

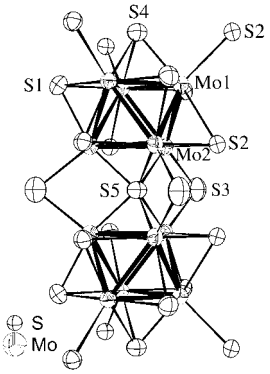

Figure 3. The $(Mo_6)_2S^i_{14}S^{i\text{-}i}S^{a\text{-}a}_3S^a_6$ unit with atomic labeling scheme. Selected distances [Å]: Mo1-Mo1 2.6921(3), Mo1-Mo2 2.6953(4), Mo2-Mo2 2.9144(4), Mo1-S1 2.4612(6), Mo1-S2 2.4655(9), Mo1-S2 2.5298(9), Mo1-S4 2.4149(11), Mo2-S1 2.4569(9), Mo2-S2 2.4691(5), Mo2-S3 2.5355(17), Mo2-S5 2.2967(3).

distorted than in the Chevrel phases with Mo–Mo distances ranging from 2.6921(3) to 2.9144(4) Å. The Mo2–Mo2 distance between the two Mo_6 clusters within the $(Mo_6)_2S^i_{14}S^{i\text{-}i}S^{a\text{-}a}_3S^a_6$ unit is 3.1264(4) Å, which is comparable to the intercluster distances observed between the Mo_6 clusters in the $M_xMo_6S_8$ compounds. The Mo–S distances range from 2.2967(3) to 2.535(2) Å. The shortest distance occurs between the Mo2 atoms and the *i*-*i* type ligand S5, and the longest one between the Mo2 atoms and the *a*-*a* type ligands S3 (Figure 3). As observed previously in the Chevrel phases, the three-dimensional arrangement of the $(Mo_6)_2S^i_{14}S^{i\text{-}i}\text{-}S^{a\text{-}a}_3S^a_6$ units arises from the sharing of the six *a*-type ligands with six *i*-type ligands. As a consequence, the connective formula of the Mo–S framework is $(Mo_6)_2S^i_8S^{i\text{-}i}S^{i\text{-}a}_{6/2}S^{a\text{-}a}_3S^{a\text{-}i}_{6/2}$. The result of this arrangement is that the shortest Mo–Mo distance between the Mo_6 clusters of adjacent $(Mo_6)_2S^i_{14}S^{i\text{-}i}\text{-}S^{a\text{-}a}_3S^a_6$ units is 3.0847(4) Å. As shown by the perspective view of the crystal structure along the *c* axis (Figure 4), the Ba2 ions reside in large channels extending along the *c* axis. The other barium atoms (Ba1) are located between two consecutive $(Mo_6)_2S^i_{14}S^{i\text{-}i}S^{a\text{-}a}_3S^a_6$ units around the threefold axis. The Ba1 cations are surrounded by ten sulfur atoms. The nearest four at about 3.1 Å form a distorted tetrahedron, and the remaining six at 3.3841(9)–3.4692(6) Å cap a face or bridge an edge. The Ba2 cations are located off-center of large cavities of twelve sulfur atoms forming an hexacapped trigonal antiprism. They are thus surrounded by nine sulfur atoms at distances between 3.394(1) and 3.734(3) Å.

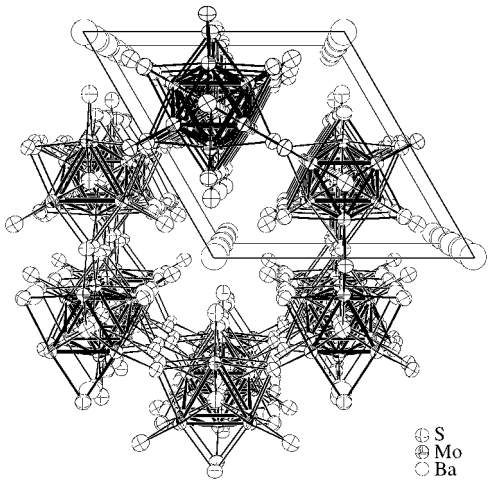

Figure 4. Perspective view of the $Ba_4Mo_{12}S_{18}$ structure down the *c* axis.

Single-crystal electrical resistivity measurements indicate that $Ba_4Mo_{12}S_{18}$ is poorly metallic, with a room-temperature resistivity of around 1 mΩ cm, and becomes a superconductor below 7 K (Figure 5). Superconductivity was also confirmed by the Meissner effect in susceptibility measurements on powder samples.

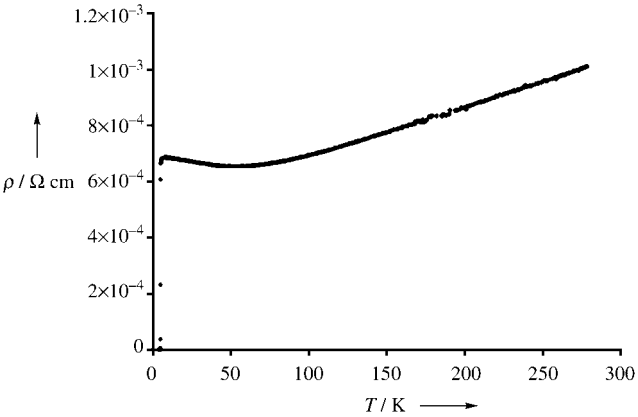

Figure 5. Temperature dependence of the electrical resistivity for a single crystal of $Ba_4Mo_{12}S_{18}$.

Metallic behavior was confirmed by periodic density functional calculations (Figure 6).[9] The Fermi level cuts a

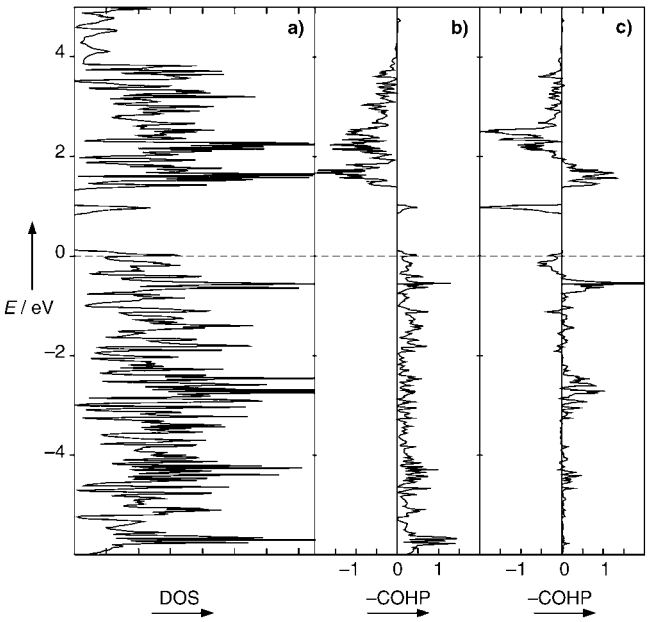

Figure 6. DFT calculations for $Ba_4Mo_{12}S_{18}$: a) total DOS, b) averaged COHP for Mo–Mo bonds of the Mo_6 unit, and c) COHP for Mo2–Mo2 bonds between the two Mo_6 clusters within the $(Mo_6)_2S^i_{14}S^{i\text{-}i}S^{a\text{-}a}_3S^a_6$ unit.

narrow peak of density of states (DOS), mainly centered on Mo atoms, that is separated by an energy gap of about 1 eV from a higher vacant DOS peak. This latter peak shows Mo2–Mo2 antibonding character (between the two Mo_6 clusters in the $(Mo_6)_2S^i_{14}S^{i\text{-}i}S^{a\text{-}a}_3S^a_6$ unit) and intra-Mo_6 Mo2–Mo2 bonding character. It is derived from a molecular orbital of the $(Mo_6)_2S^i_{14}S^{i\text{-}i}S^{a\text{-}a}_3S^a_6$ unit which is the out-of-phase combination that results from interaction of the same MO of each Mo_6 cluster among the twelve Mo–Mo bonding and nonbonding MOs.[10] The vacancy of the band derived from this MO explains the rather long intra-Mo_6 Mo2–Mo2 contacts of 2.9144 Å. Since the optimal number of metallic electrons (ME) for an $Mo_6S^i_8S^a_6$ octahedral cluster is 24,[10] that for such an $(Mo_6)_2$ unit is therefore $24+24-2=46$. Analysis of the integrated crystal orbital Hamiltonian populations (COHP)[11] indicates that the Mo2–Mo2 bond strength between the Mo_6 clusters is about half that of the Mo–Mo bonds within the Mo_6 unit. Therefore, the Mo_{12} cluster must be regarded as the structural unit of this compound, and not Mo_6. Considering that the ME count for the Mo_{12} unit in $Ba_4Mo_{12}S_{18}$ is 44, and because of the overall Mo–Mo nonbonding character of the DOS at the Fermi level, it should be possible to reduce this compound without altering its structural arrangement and make it semiconducting by adding two extra electrons.

Experimental Section

Preparation of $Ba_4Mo_{12}S_{18}$: Single-phase powder of $Ba_4Mo_{12}S_{18}$ was obtained from the required stoichiometric mixture of MoS_2, BaS, and Mo. These powders were mixed, ground together in a mortar, and then cold-pressed in a hand press. The pellet was loaded into a molybdenum crucible, which was sealed under a low argon pressure with an arc-welding system. The crucible was heated at 300 °C h^{-1} to 1500 °C and held there for four days, then cooled at 100 °C h^{-1} to 1100 °C, and finally furnace-cooled to room temperature.

Electrical resistivity and magnetic susceptibility measurements: The ac resistivity was measured out on a single crystal by a standard four-probe technique between 290 and 4.2 K. Ohmic contacts were made by attaching molten indium ultrasonically. Magnetic susceptibility data of $Ba_4Mo_{12}S_{18}$ were collected on a SHE-906 SQUID magnetosusceptometer under a magnetic field of 20 G.

Crystal data for $Ba_4Mo_{12}S_{18}$: hexagonal, space group $P6_3/mmc$ (no. 194), $a=10.6985(1)$, $c=14.2264(2)$ Å, $V=1410.17(3)$ Å^3, $Z=2$, $\rho_{calcd}=5.362$ Mg m^{-3}, $F(000)=2032$, $\lambda(Mo_{K\alpha})=0.71073$ Å, $\mu(Mo_{K\alpha})=11.938$ mm^{-1}, $T=20$ °C. A black hexagonal crystal of approximate dimensions $0.10\times0.08\times0.05$ mm was employed in the collection of intensity data on a Nonius KappaCCD diffractometer. Reflection indexing, correction for Lorentzian and polarization effects, peak integration, and background determination were performed by using the EvalCCD program.[12] An absorption correction was applied by using the description of the crystal faces.[13] Of 35551 reflections collected in the $\theta=2.62$–42.0° range, 1877 were independent ($R_{int}=0.0493$). The structure was solved by direct methods with the program SIR97[14] and refined on F by using JANA2000.[15] Refinement of the occupancy factor of the Ba2 atoms located along the z axis around the point (0,0,0.5) yielded a value of 0.502(4), which hence was fixed to 0.5. This model was refined with harmonic anisotropic atomic displacement parameters for all atoms down to $R=0.0275$. At this stage, a difference Fourier synthesis revealed the highest residual peaks in the vicinity of the Ba2 site alternating with negative regions. Subsequently, a Gram–Charlier expansion of the nonharmonic atomic displacement parameters up to the fourth order was used in the refinement for the Ba2 atom. Such refinement reduced the R factor from 0.0275 to 0.0235, and the residual peaks from 11.44 and -5.70 e Å^{-3} to 1.55 and -0.98 e Å^{-3}. Because of the disorder of the Ba2 atoms, we performed reciprocal-space reconstruction of different planes, as well as long-exposure rotations about the a and c axes on a single crystal on the KappaCCD diffractometer. In both cases, we did not observe any superlattice reflection or diffuse line. Further details on the crystal structure investigations may be obtained from the Fachinformationszentrum Karlsruhe, 76344 Eggenstein-Leopoldshafen, Germany (fax: (+49) 7247-808-666; e-mail: crysdata@fiz-karlsruhe.de), on quoting the depository number CSD-414217.

Calculations: Self-consistent ab initio band-structure calculations were performed on a model compound of $Ba_4Mo_{12}S_{18}$ with the scalar relativistic tight-binding linear muffin-tin orbital (LMTO) method in the atomic-spheres approximation including the combined correction.[9] Exchange and correlation were treated in the local density approximation using the von Barth–Hedin local exchange correlation potential.[16] Charge self-consistency and the average properties were obtained from 57 irreducible k points.

Received: July 9, 2004
Revised: November 11, 2004
Published online: January 20, 2005

Keywords: barium · cluster compounds · molybdenum · solid-state structures · superconductors

[1] Ø. Fischer, *Appl. Phys.* **1978**, *16*, 1.
[2] K. Yvon, *Curr. Top. Mater. Sci.* **1979**, *3*, 53.
[3] *Superconductivity in Ternary Compounds, Vols. I, II* (Eds.: Ø. Fischer, M. B. Maple), Springer, Berlin, **1982** (*Top. Curr. Phys.* **1982**, 32).
[4] R. Flukiger in *Superconductor Materials Science* (Eds.: S. Foner, B. Schwartz), Series B, Plenum, New York, **1981**, pp. 511–604.
[5] J. Guillevic, O. Bars, D. Grandjean, *J. Solid State Chem.* **1973**, *7*, 158.
[6] H. Schäfer, H.-G. von Schnering, *Angew. Chem.* **1964**, *76*, 833.
[7] C. Perrin, M. Sergent, *J. Less-Common Met.* **1986**, *123*, 117.
[8] S. Picard, J.-F. Halet, P. Gougeon, M. Potel, *Inorg. Chem.* **1999**, *38*, 4422.
[9] a) O. K. Andersen, *Phys. Rev. B* **1975**, *12*, 3060; b) H. L. Skriver, *The LMTO Method*, Springer, Berlin, **1984**.
[10] T. Hughbanks, R. Hoffmann, *J. Am. Chem. Soc.* **1983**, *105*, 1150.
[11] R. Dronskowski, P. E. Blöchl, *J. Phys. Chem.* **1993**, *97*, 8617.
[12] A. J. M. Duisenberg, PhD thesis, University of Utrecht (The Netherlands), **1998**.
[13] J. de Meulenaar, H. Tompa, *Acta Crystallogr. Sect. A* **1965**, *19*, 1014.
[14] A. Altomare, M. C. Burla, M. Camalli, G. L. Cascarano, C. Giacovazzo, A. Guagliardi, A. G. G. Moliterni, G. Polidori, R. Spagna, *J. Appl. Crystallogr.* **1999**, *32*, 115.
[15] V. Petricek, M. Dusek, Jana2000, Institute of Physics, Academy of Sciences of the Czech Republic, Prague, Czech Republic, **2000**.
[16] U. von Barth, L. Hedin, *J. Phys. C* **1972**, *5*, 1629.

